



Contents lists available at ScienceDirect

# Bioorganic & Medicinal Chemistry Letters

journal homepage: [www.elsevier.com/locate/bmcl](http://www.elsevier.com/locate/bmcl)

## Anti-tumor activity evaluation of novel chrysin–organogermanium(IV) complex in MCF-7 cells

Fen Yang<sup>a</sup>, Hua Jin<sup>a</sup>, Jiang Pi<sup>a</sup>, Jin-huan Jiang<sup>a</sup>, Li Liu<sup>a</sup>, Hai-hua Bai<sup>a</sup>, Pei-hui Yang<sup>a</sup>, Ji-Ye Cai<sup>a,b,\*</sup><sup>a</sup>Department of Chemistry of Jinan University, Guangzhou 510632, China<sup>b</sup>State Key Laboratory of Quality Research in Chinese Medicines, Macau University of Science and Technology, Macau 000853, China

### ARTICLE INFO

#### Article history:

Received 25 June 2013

Revised 24 July 2013

Accepted 13 August 2013

Available online 19 August 2013

#### Keywords:

Chrysin

Chry–Ge

MCF-7

Atomic force microscopy (AFM)

### ABSTRACT

Chrysin (5,7-dihydroxyflavone, Chry) is a natural product extracted from plants, honey, and propolis. In this work, a novel chrysin–organogermanium(IV) complex (Chry–Ge) with enhanced anticancer activities was synthesized, and its potential anticancer effects against cancer cells were measured using various methods. MTT results showed that Chry–Ge had significant inhibition effects on the proliferation of MCF-7, HepG2 and Colo205 human cancer cell lines in a dose-dependent manner while had little cytotoxic effects on MCF-10A human normal cells (MCF-10A cells) with the same treatment of Chry–Ge. These results suggested that Chry–Ge possessed enhanced anticancer effects and high selectivity between cancer cells and normal cells. The immuno-staining results showed that the nuclei of MCF-7 cells represented a total fragmented morphology and a disorganized cytoskeletal network in MCF-7 cells after Chry–Ge treatment. Besides, atomic force microscopy (AFM) was applied to detect the changes of ultrastructural and biomechanical properties of MCF-7 cellular membrane induced by Chry–Ge. The AFM data indicated that Chry–Ge treatment directly caused the decrease of cell rigidity and adhesion force of MCF-7 cells, suggesting that membrane toxicity might be one of the targets for Chry–Ge in MCF-7 cells. Moreover, the fluorescence-based flow cytometric analysis demonstrated that Chry–Ge could induce apoptosis in MCF-7 cells in ROS-dependent mitochondrial pathway. All results collectively showed that Chry–Ge could be as a promising anticancer drug for cancer therapy.

© 2013 Elsevier Ltd. All rights reserved.

Cancer has become an enormous global health burden, because there are about 12.7 million cancer cases and 7.6 million cancer deaths every year based on the estimation of Globocan in 2008.<sup>1,2</sup> During the past decades, chemotherapy has been regarded as the most effective method for cancer therapy, but most of cancer patients are also suffering from the toxicity and side effects induced by chemotherapy. Thus, to design and develop new drugs with high efficacy to fight against cancer cells is a big challenge of vital importance for human health.

Chrysin (5,7-dihydroxyflavone, Chry) is a natural product extracted from plants, honey, and propolis. A lot of researches have shown that chrysin has a broad spectrum of biological and pharmacological properties, such as anti-inflammation, anti-oxidation and protective effects.<sup>3–6</sup> Recently, it has also been proved that chrysin obtains the ability to inhibit proliferation and induce apoptosis in cancer cells, making it a potential candidate as anticancer drug.<sup>6,7–19</sup>

Germanium (Ge) is considered to play a key role in the pharmacological effects of some medicinal plants. Compared with the

inorganic germanium compounds, organic germanium compounds have much lower toxicity, and particularly, it can even enhance immunity of animal models.<sup>20,21</sup> In our previous study, we have proved that Ge(IV)–polyphenol complexes can inhibit the proliferation of HepG2 cells through arresting cell cycle and disrupting the morphology of HepG2 cells, achieving potential anticancer activities.<sup>22</sup> Poly-*trans*-[(2-carboxyethyl)germasquioxane] (Ge-132), which is the most common and well-studied organic germanium compound, has also been reported to possess anticancer effects and enhance immunity.<sup>23–25</sup>

In the present study, we demonstrated a simple method to synthesize Chry–Ge complex through the reaction between chrysin and triphenylgermanium bromide (Fig. 1A). The Supplementary data Figure S1 showed the chemical structure formula of Chry–Ge. FT-IR and elementary analysis were performed to verify the formation of Chry–Ge complex. The FT-IR spectra data of Chry–Ge (Fig. 1B) showed a clear absorbance peak at 859.4 cm<sup>-1</sup>, while no similar special absorbance peaks were found in the spectra of triphenylgermanium bromide and chrysin in this region. In addition, the appearance of a new peak was observed for the stretching vibration of Ge–O, whereas no obvious shift was observed for the groups of C–O–H, C–H, and C=O in the spectra of Chry–Ge complex. The elementary analysis results (Fig. 1C)

\* Corresponding author at: Department of Chemistry of Jinan University, Guangzhou 510632, China. Tel./fax: +86 020 85223569.

E-mail address: [tyjcai@jnu.edu.cn](mailto:tyjcai@jnu.edu.cn) (J.-Y. Cai).

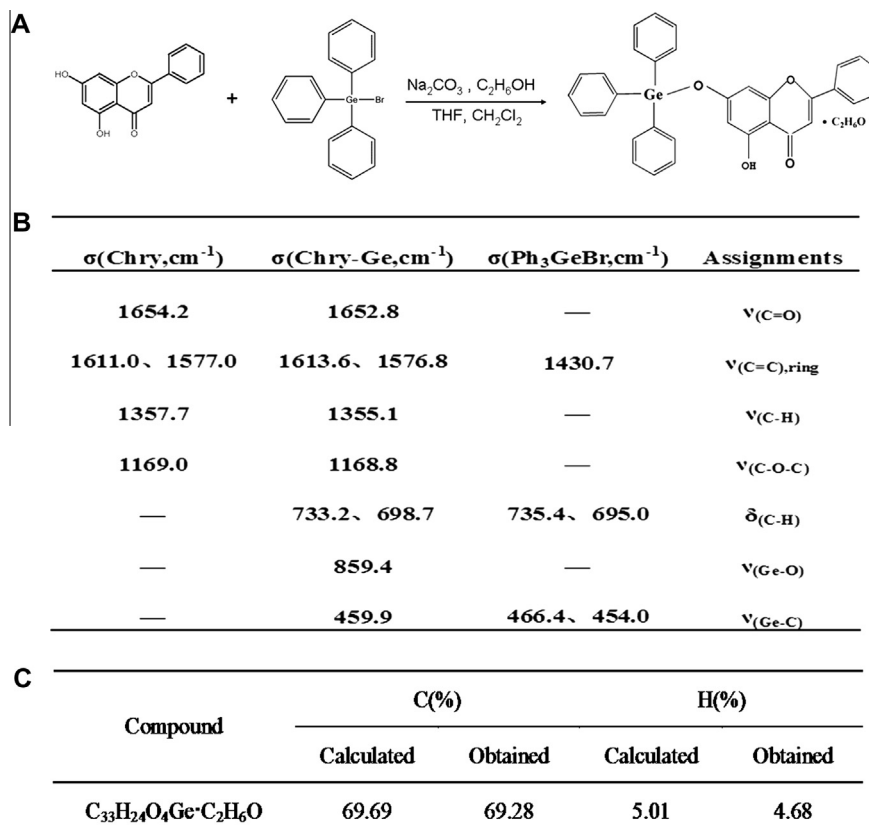


**Figure 1.** (A) Schematic representation of the synthesis of Chry-Ge. (B) The dates of FT-IR spectral of triphenylgermanium bromide, chrysin and Chry-Ge complex. (C) Dates of elementary analysis of Chry-Ge.

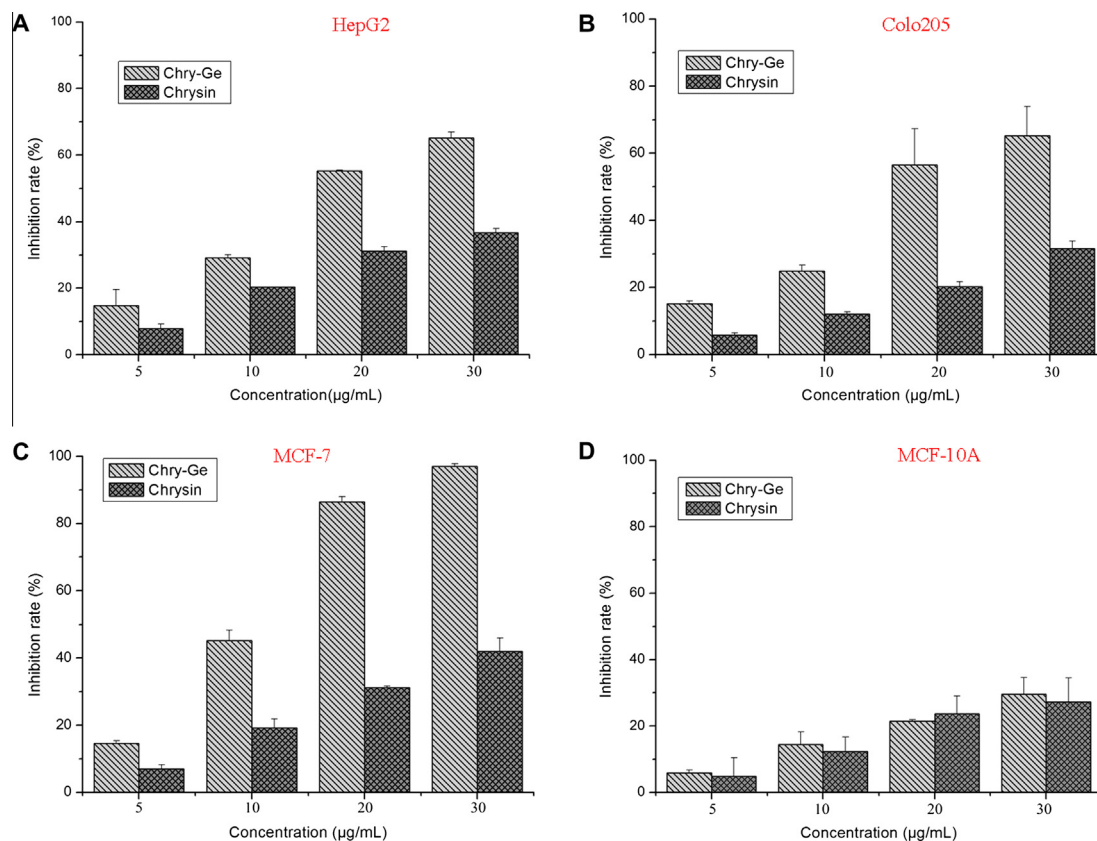


**Figure 2.** Cell viability was determined by a colorimetric MTT assay. Growth inhibition of Chry-Ge or Chrysin on (A) HepG2, (B) Colo205, (C) MCF-7, and (D) MCF-10A.

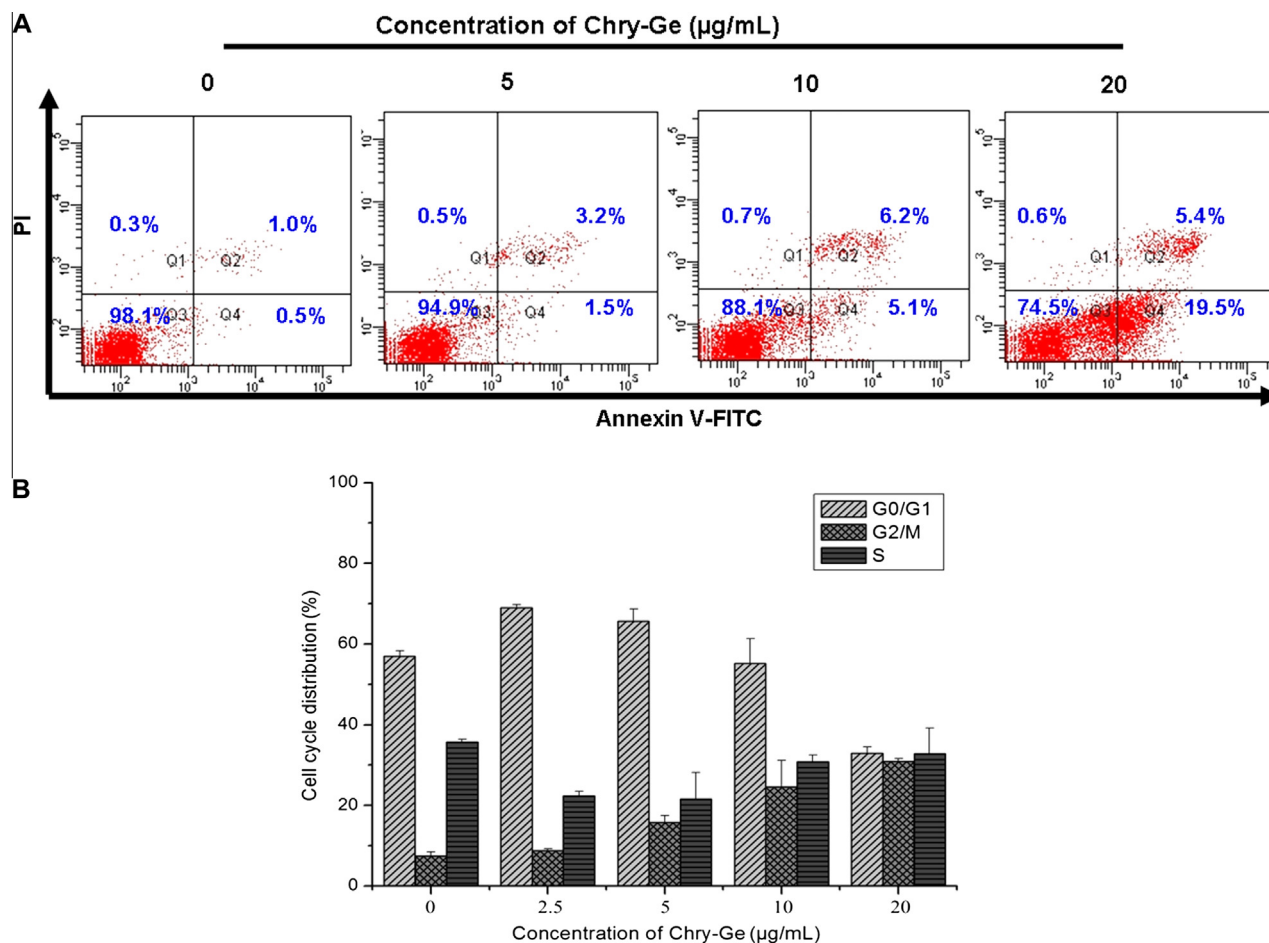


**Figure 3.** (A) Flow cytometric analysis of Chry-Ge induced apoptosis in MCF-7 cells using annexin-V-FITC/PI. Quadrants: Q3: live cells; Q4: apoptotic cells; Q2: necrotic or late apoptotic cells. (B) Cell cycle distribution of MCF-7 cells before and after treatments with Chry-Ge for 24 h detected by PI-based flow cytometry.

showed that the theoretical results of H (5.01%) and C (69.69%) element contents in Chry-Ge complex were in good agreement with the experimental results of H (4.68%) and C (69.28%). To further verify the formation of Chry-Ge complexes,  $^1\text{H}$  NMR and  $^{13}\text{C}$  NMR (Bruker, USA) were performed and the data were showed in the [Supplementary data](#) ( $^1\text{H}$  NMR (Table 2),  $^{13}\text{C}$  NMR (Table 3)). These results demonstrated the successful preparation of Chry-Ge complex. To ensure the purity of Chry-Ge complex, re-crystallization was used to purify the production.

To detect the biological activities of Chry-Ge, MTT assay was performed firstly to evaluate the inhibition effects on proliferation of cancer cells and normal cells. The data in [Figure 2](#) showed that both Chry-Ge and chrysin could effectively inhibit the growth and proliferation of cancer cells in a dose-dependent manner, including MCF-7, HepG2 and Colo205 cells ([Fig. 2](#)). Notably, the inhibition effects of Chry-Ge were much stronger than that of Chrysin, demonstrating the enhancement of anticancer activities of Chrysin after the coupling with germanium. But interestingly, both Chry-Ge and chrysin showed much lower toxicity against MCF-10A cells, a normal human breast cell lines (shown in [Fig. 2D](#)). The inhibition rates of HepG2, Colo205, MCF-7, and MCF-10A cells induced by both Chry-Ge and chrysin, respectively, were demonstrated in the [Supplementary data Table 4](#).

These results suggested that Chry-Ge compound possessed much higher anticancer activity compared with chrysin and showed similar low toxicity against normal cells, showing higher selectivity killing effect against cancer cells.

Annexin-V Apoptosis Detection Kit is based on the observation of membrane phosphatidylserine (PS) from the inner face of the plasma membrane to the cell surface when cells are suffering from apoptosis.<sup>26</sup> [Figure 3](#) showed the mean apoptotic population of MCF-7 cells, which were 0.5%, 1.5%, 5.1% and 19.5% for control, 5, 10 and 20  $\mu\text{g/mL}$  Chry-Ge treated MCF-7 cells (24 h), respectively. The results strongly suggested that Chry-Ge possessed high apoptotic induction effect in cancer cells, especially in high dosages.

Cell cycle consists of four distinct phases: G1 phase (cell growth), S phase (DNA synthesis), G2 phase (cell division) and M phase (mitosis and DNA replication). To further detect the alterations in cell cycle induced by Chry-Ge, MCF-7 cell cycle was investigated by flow cytometry using PI staining after 24 h of Chry-Ge treatment. It was found that the average percentage of cells in G2 phase increased from  $7.43 \pm 0.98\%$  to  $8.73 \pm 0.45\%$ ,  $15.8 \pm 1.68\%$ ,  $24.5 \pm 6.61\%$ , and  $30.9 \pm 0.64\%$  after 0, 2.5, 5, 10, and 20  $\mu\text{g/mL}$  Chry-Ge treatments, respectively ([Fig. 3B](#)). It suggested that Chry-Ge treatment could arrest MCF-7 cells in G2/M phase, which might due to the destruction of DNA replication and mitosis processes of MCF-7 cells after Chry-Ge treatment.

Besides, high levels of reactive oxygen species (ROS) can cause cellular damage owing to the duration of ROS stress to mediate apoptosis by regulating the expression of various apoptosis regulatory proteins.<sup>27</sup> To determine if ROS were involved in Chry-Ge induced apoptosis, we examined the cellular ROS production in response to Chry-Ge exposure by flow cytometry. As shown in [Figure 4](#), the results implied that mean fluorescence intensity

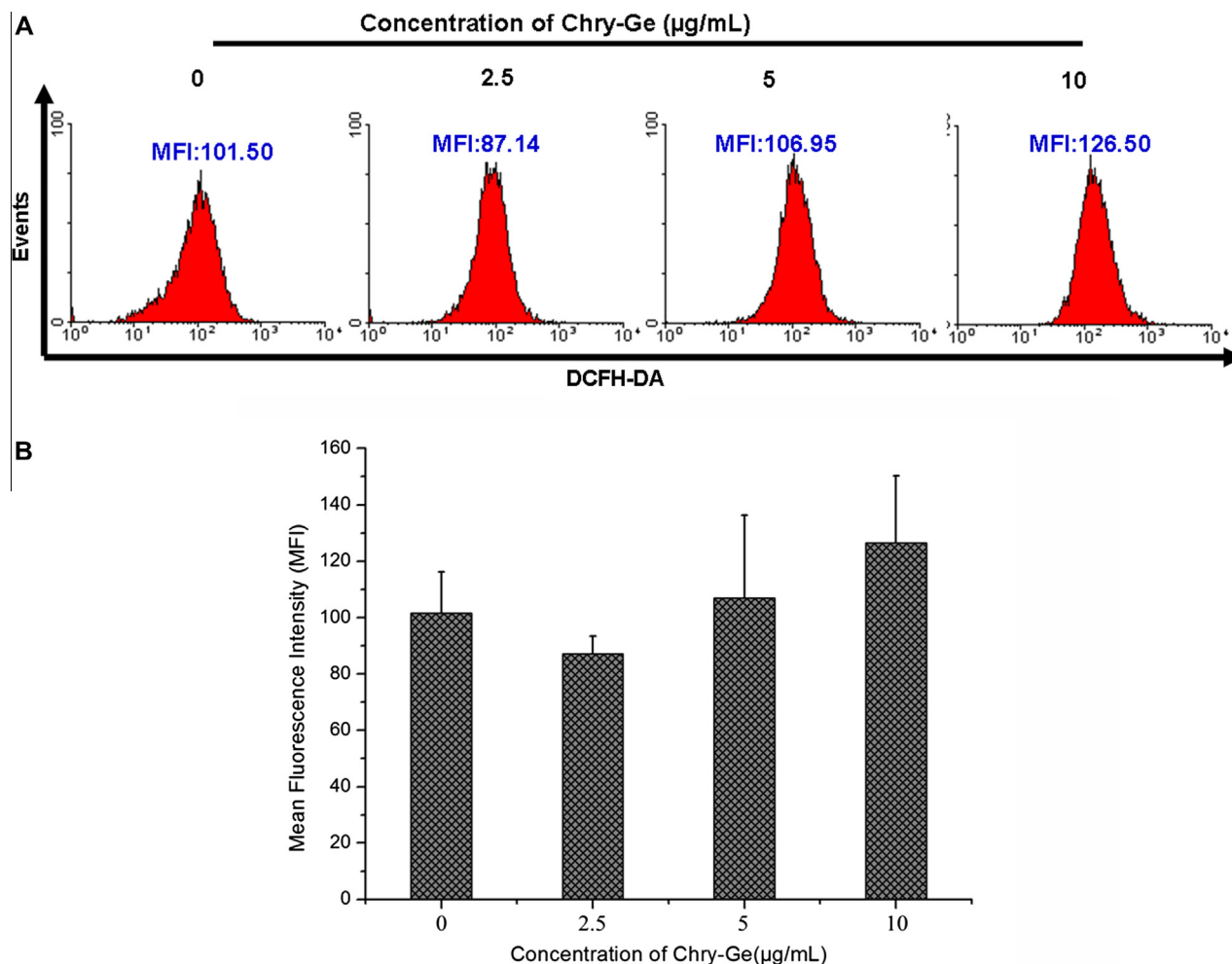


**Figure 4.** Flow cytometric analysis of ROS levels in designated concentrations Chry-Ge treated MCF-7 cells. (A) Changes of ROS levels in Chry-Ge treated MCF-7 cells. (B) The data in B represents three separated experiments.

(MFI) of DCFH-DA in Chry-Ge treated MCF-7 cells ranged from 101.50 to 126.50. After low concentration of Chry-Ge treatment, ROS levels decreased, which was responsible for the removing of free radicals by Chry-Ge at low dosage. But the ROS levels were increased after the treatment of high dosage of Chry-Ge, showing that why high concentration of Chry-Ge could induce remarkable apoptosis in MCF-7 cells.

In this work, rhodamine 123 (Rh123) was used to detect mitochondrial membrane potential (MMP) as a quantitative method.<sup>28</sup> Figure 5 showed that mean fluorescence intensity (MFI) of Rh123 was decreased from 3094 for control cells to 483 for MCF-7 cells treated with Chry-Ge. These results demonstrated that Chry-Ge could induce MMP disruption in MCF-7 cells.

The loss of MMP would lead to the release of cytochrome c, the activation of caspase, and the initiation of apoptotic cascades.<sup>29–31</sup> In order to confirm the apoptosis pathway, we also tested the activity of caspase 3/8/9, which were central initiators and executors of the apoptotic process.<sup>32</sup> The results showed that low dosages of Chry-Ge could not activate caspases while high dosages of Chry-Ge remarkably activate caspase proteins (Fig. 6). Especially, after 20 µg/mL Chry-Ge treatment, the activities of caspase-3, caspase-8 and caspase-9 increased from 100% to 214.5%, 181.1% and 286.0%, respectively. These results showed that Chry-Ge induced apoptosis in MCF-7 cells with the involvement of caspase-3, caspase-8 and caspase-9 activation. Taken the result obtained above together, it collectively indicated that Chry-Ge could

induce the apoptosis in MCF-7 cells mainly through ROS-related mitochondrial pathway.

Roughly 70% of all patients dying of breast cancer have bone metastases.<sup>33</sup> Therefore, we also performed wounding-healing experiments to detect the effects of Chry-Ge on migration of MCF-7 cells.

The potency in movements and invasions of MCF-7 cells (Fig. 7) were examined by scratching the MCF-7 cells, which showed that the healing of scratched MCF-7 breast cancer cells was delayed with the treatment of Chry-Ge. The results showed that enhanced migration of MCF-7 cells and complete wound closure by 24 h was observed in plates, while a significant area of the wound remained uncovered in Chry-Ge treated group compared to the control. This suggested that Chry-Ge was able to significantly block the MCF-7 cell migration. Besides, for further confirm the effects of Chry-Ge on migration of normal cells, MCF-10A cells were used as a model in wounding-healing assays. As shown in Supplementary data Figure S5, there was a little inhibition effect on migration of MCF-10A cells induced by Chry-Ge.

In addition, apoptosis is characterized by a series of stereotypic morphological changes such as formation of apoptotic bodies, nuclear and cytoplasmic condensation, chromatin fragmentation, shrinkage of cells and bleb formation.<sup>34</sup> Previous reports have provided evidence that cytoskeleton alterations can induce apoptosis as well as necrosis in a variety of model.<sup>35,36</sup> Thus, it is very important to investigate whether Chry-Ge has effects on the

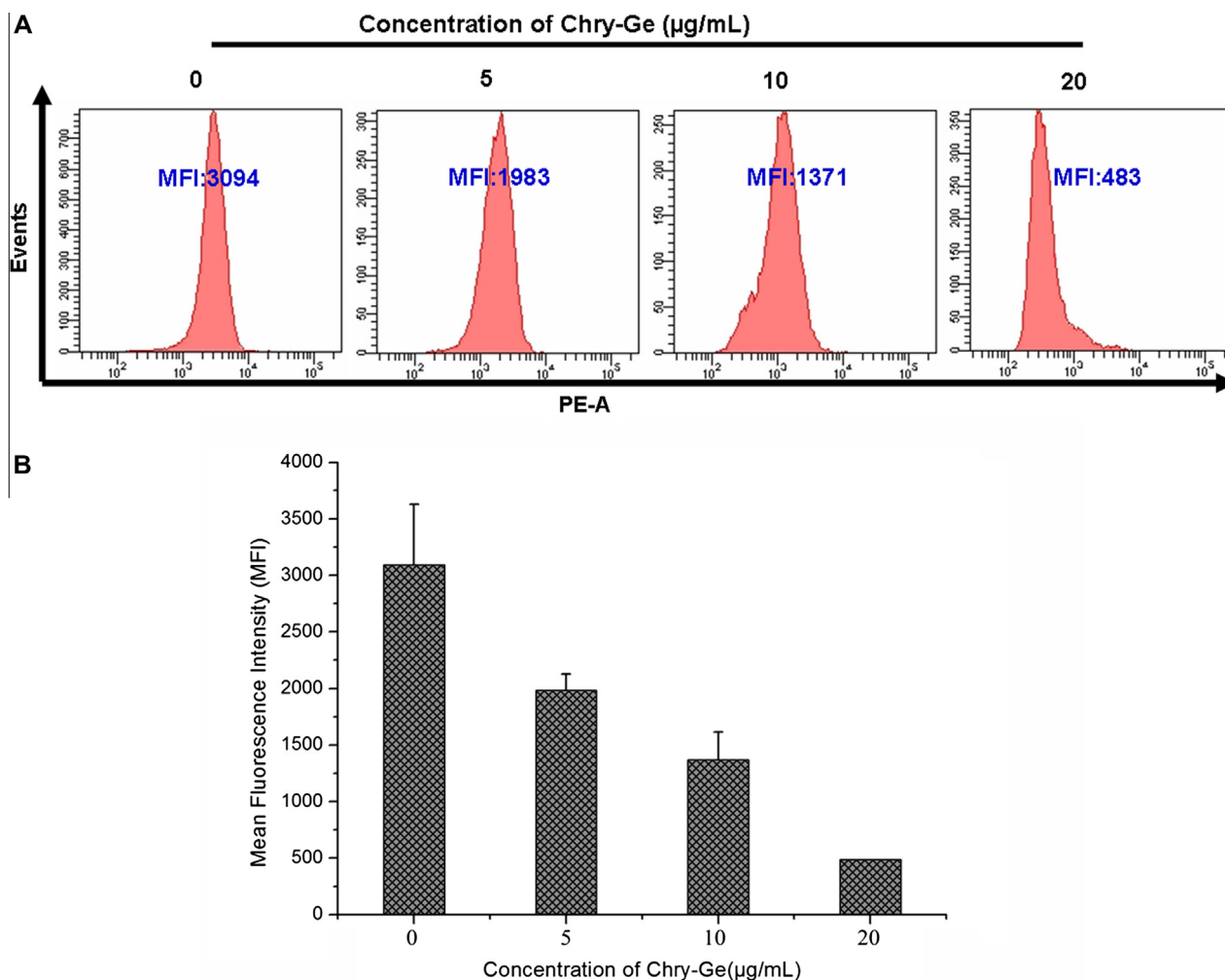


**Figure 5.** Flow cytometric analysis of MMP in designated concentrations Chry-Ge treated MCF-7 cells. (A) Changes of MMP in Chry-Ge treated MCF-7 cells. (B) The data in B represents three separated experiments.

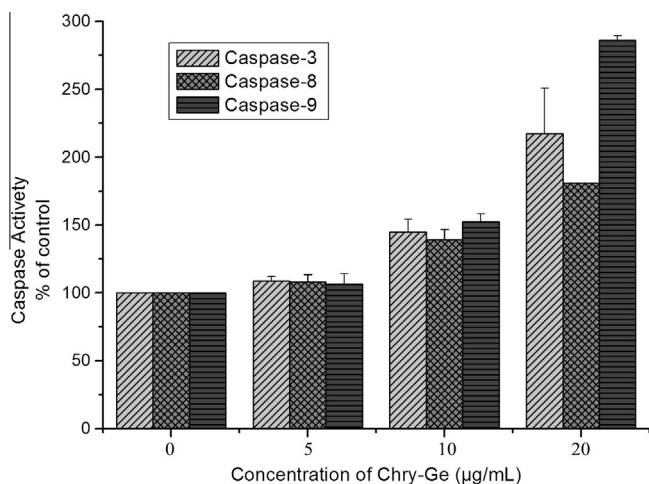


**Figure 6.** Caspase-3, caspase-8 and caspase-9 activity were measured with whole cell extracts by a fluorometric method. All data were expressed as mean values  $\pm$  standard deviation from three independent experiments.

arrangement of cytoskeleton or not. [Figure 8](#) showed the reorganization of  $\alpha$ -tubulin of MCF-7 cells stained with Tubulin-Tracker

red. The assembly of tubulin fibres in control cells represented regular mesh networks ([Fig. 8A–F](#)) while these microfilaments disrupted after Chry-Ge treatments, which also induced the damage of cell integrity ([Fig. 8C](#)). Also, the alterations in cytoskeleton in MCF-10A cells induced by Chry-Ge were detected. As shown in [Supplementary data Figure S6](#), there were not significant changes in the cytoskeleton of MCF-10A cells after treated with 10  $\mu\text{g/mL}$  of Chry-Ge, which indicated that Chry-Ge almost did not cause damages to the cytoskeleton of MCF-10A cells.

To further investigate how Chry-Ge induced changes in the morphology of nuclei, DAPI specific staining experiments were performed. When DAPI bind to natural double-stranded DNA, the fluorescence is strongly enhanced so that the morphology of the nuclei can be clearly visualized and the apoptotic cells can be identified. [Figure 8G–L](#) revealed the typical nuclei morphology in DAPI-stained control MCF-7 cells and 10  $\mu\text{g/mL}$  Chry-Ge treated MCF-7 cells. Control MCF-7 cells showed intact and plump nuclei ([Fig. 8G](#)). But the nuclei of apoptotic MCF-7 cells induced by Chry-Ge represented the segmentation of nuclei and the gathering of condensed chromatin at the periphery of the nuclear membrane ([Fig. 8J](#)). Taken together, these results indicated that Chry-Ge could significantly change the nuclei morphology of MCF-7 cells through induction of apoptosis in MCF-7 cells.

The cell membrane forms a barrier between the cell and the external environment, and acts as the exchange interface of

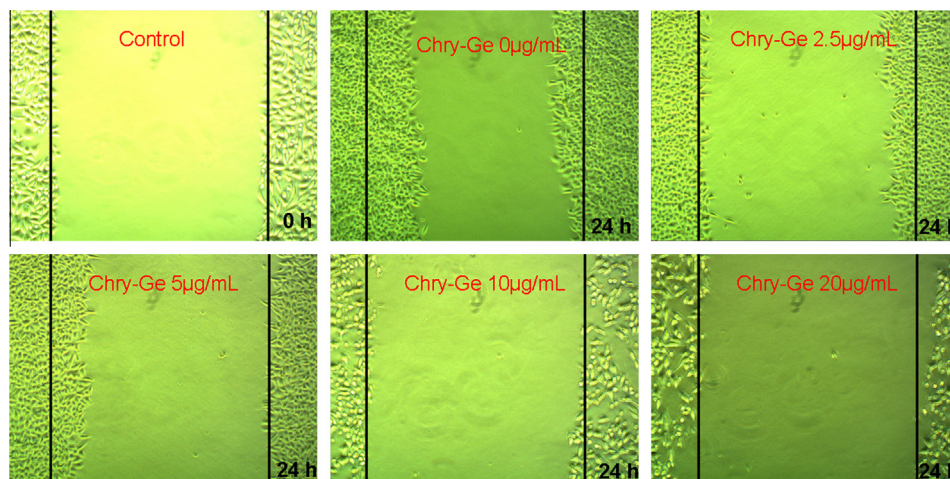


**Figure 7.** Effects of Chry-Ge on MCF-7 migration in scratching assays. Cells were wounded with p200 pipet tip in the presence or absence of Chry-Ge, respectively. Images were acquired at 0 and 24 h in scratching assay. The solid line of each picture was artificial, and the distance between the two lines was equal.

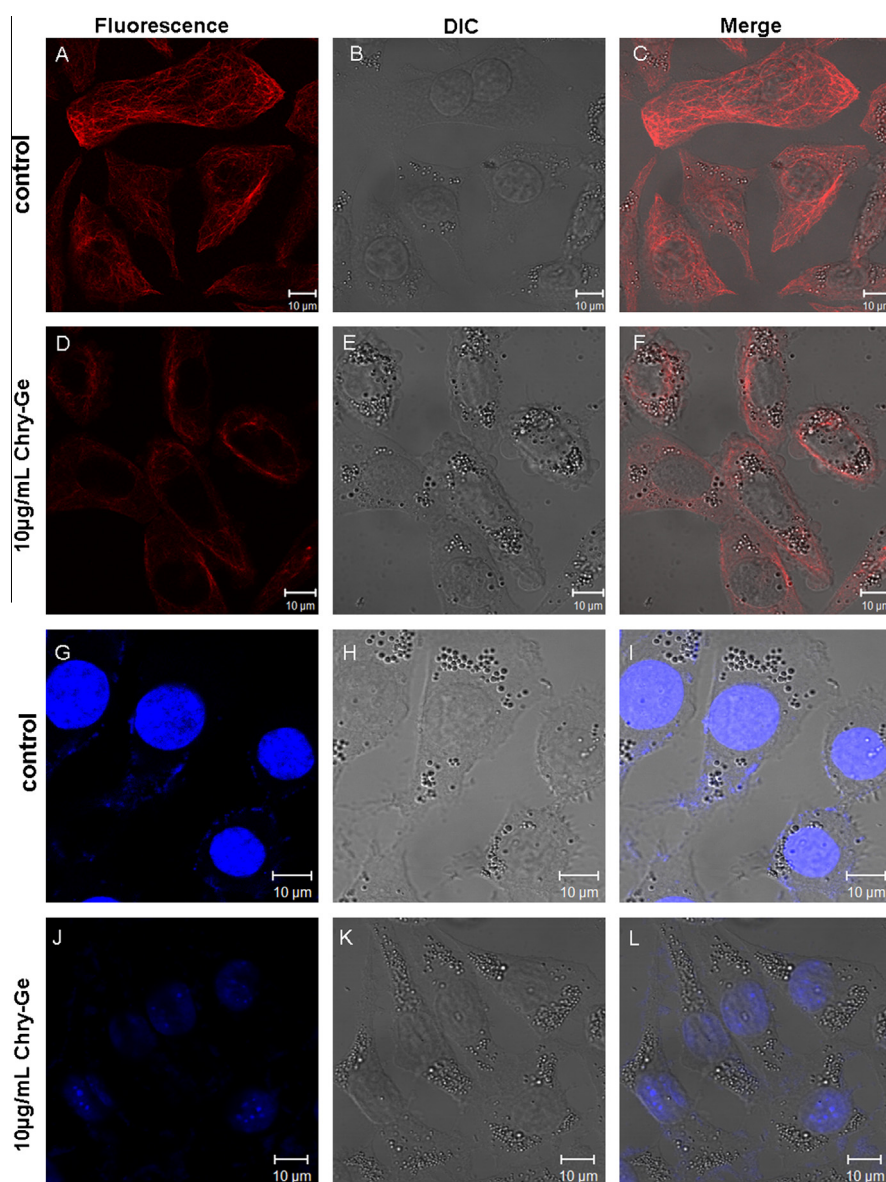


**Figure 8.** Immunofluorescent data of MCF-7 cells treated with different concentrations of Chry-Ge. (A–F) Reorganization of cytoskeleton in cells stained with  $\alpha$ -tubulin. (G–L) Nuclei of normal and apoptotic cells stained with DAPI.

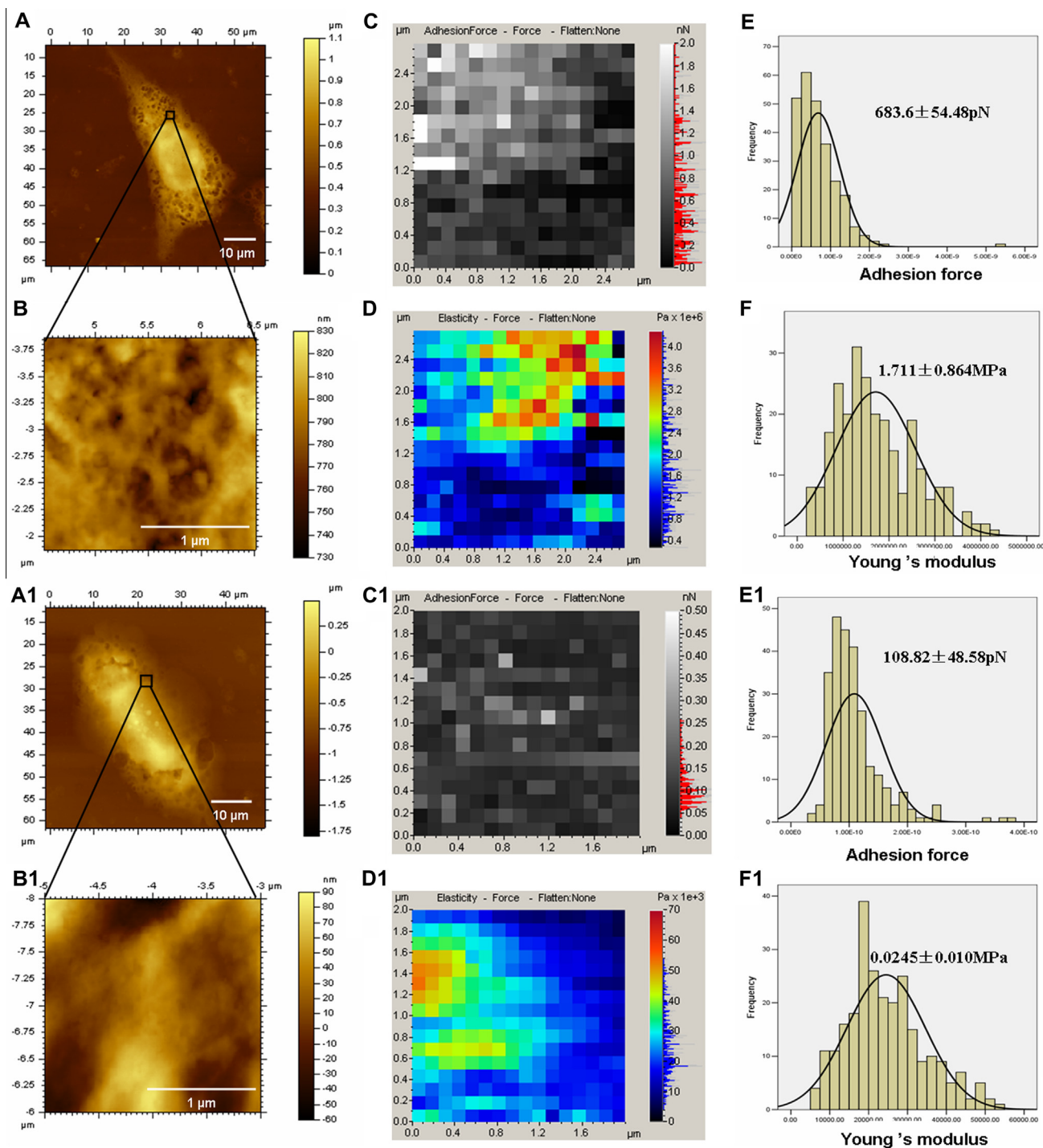


**Figure 9.** AFM force measurements of control MCF-7 cells (A–F) and MCF-7 cells treated with 10 µg/mL Chry-Ge (A1–F1). (C, C1) Adhesive force maps extracted and reconstructed from the force–distance curves measured at different spots ( $n = 256$ ) on cell surfaces. (E, E1) Histograms and corresponding GAUSSIAN distributions of cell-surface adhesion force. (D, D1) Young's modulus maps extracted and reconstructed from the force–distance curves measured at different spots ( $n = 256$ ) on cell surfaces. (F, F1) Histograms and corresponding GAUSSIAN distributions of Young's modulus. Scanning area: (A)  $60 \times 60 \mu\text{m}^2$ , (B)  $2 \times 2 \mu\text{m}^2$ , (A1)  $50 \times 50 \mu\text{m}^2$ , (B1)  $2 \times 2 \mu\text{m}^2$ .

materials between the cell inside and external environment.<sup>37</sup> Thus, the changes in cell membrane structure can be a sensitive indicator of the growth status for cells. As a nondestructive cell surface imaging tool, atomic force microscopy (AFM) could provide us a lot of information about morphological, ultrastructural and mechanical changes in cell-surface topography at nanoscale.<sup>37,38</sup> In this work, AFM were employed to detect the changes in morphology, ultrastructure and biomechanical properties of MCF-7 cells induced by Chry-Ge treatment. The high-resolution AFM

topographical images showed that surface morphology and membrane ultrastructure of MCF-7 cells changed after the treatment of Chry-Ge (Fig. 9). It was demonstrated that control MCF-7 cells had oval shape with an obvious nucleus region at the centre of cells, and the cell membrane was relatively intact (Fig. 9A, B). But the Chry-Ge treated MCF-7 cells were deformed with shrunk cell tails (Fig. 9A1, B1). The AFM force measurements revealed that upon Chry-Ge treatments, the tip-cell adhesion force decreased from  $683.6 \pm 54.48$  pN (Fig. 9E) to  $108.8 \pm 48.58$  pN (Fig. 9E1) and the

Young's modulus decreased from  $1.711 \pm 0.864$  MPa (Fig. 9F) to  $0.0245 \pm 0.010$  MPa (Fig. 9F1). These changes were clearly showed in the adhesion force maps and Young's modulus maps (Fig. 9C, C1, D, D1) corresponding to an area of  $2 \times 2 \mu\text{m}^2$  on cell surface (Fig. 9B, B1). These results indicated that Chry–Ge could induce the damage of MCF-7 morphology and the changes of cell membrane mechanical properties.

In summary, this work indicated that Chry–Ge could significantly inhibit the proliferation and growth of cancer cells with high selectivity between cancer cells and normal cells. We then studied the cytotoxic effects of Chry–Ge on MCF-7 cells and investigated the mechanism responsible for these effects. Chry–Ge could effectively induce cell cycle arrest in G2/M phase and induce apoptosis through induction of intracellular ROS level, disruption of MMP and activation of caspase 3/8/9 in MCF-7 cells. Meanwhile, the morphological and mechanical changes in the MCF-7 cells detected by AFM at nano-scale demonstrated that Chry–Ge could disrupt the cell morphology and change the mechanical properties of cell membrane in MCF-7 cells. These findings collectively suggested that Chry–Ge could be as a potential candidate for the further development of anticancer drugs.

### Acknowledgements

This work was supported by research grants from Science and Technology 973, China (No.2010CB833603), Overseas, Hong Kong & Macao Cooperative Research Funds of China (No.31129002) and the National Natural Science Foundation of China (No.21071064).

### Supplementary data

Supplementary data associated with this article can be found, in the online version, at <http://dx.doi.org/10.1016/j.bmcl.2013.08.055>.

### References and notes

1. Ferlay, J.; Shin, H. R.; Bray, F.; Forman, D.; Mathers, C.; Parkin, D. M. *Int. J. Cancer* **2010**, *127*, 2893.
2. Jemal, A.; Bray, F.; Center, M. M.; Ferlay, J.; Ward, E.; Forman, D. *CA Cancer J. Clin.* **2011**, *61*, 69.
3. Lim, H.; Jin, J. H.; Park, H.; Kim, H. P. *Eur. J. Pharmacol.* **2011**, *670*, 617.
4. Anand, K. V.; Anandhi, R.; Pakkiyaraj, M.; Geraldine, P. *Toxicol Ind Health.* **2011**, *27*, 923.
5. Ciftci, O.; Ozdemir, I. *Immunopharmacol. Immunotoxicol.* **2011**, *33*, 504.
6. Khan, R.; Khan, A. Q.; Qamar, W.; Lateef, A.; Tahir, M.; Rehman, M. U.; Ali, F.; Sultana, S. *Toxicol. Appl. Pharmacol.* **2012**, *258*, 315.
7. Zhang, T.; Chen, X.; Qu, L.; Wu, J.; Cui, R.; Zhao, Y. *Bioorg. Med. Chem. Lett.* **2004**, *12*, 6097.
8. von-Brandenstein, M. G.; Ngum-Abety, A.; Depping, R.; Roth, T.; Koehler, M.; Dienes, H. P.; Fries, J. W. U. *Biochim. Biophys. Acta, Mol. Cell Res.* **2008**, *1783*, 1613.
9. Woo, K. J.; Jeong, Y. J.; Park, J. W.; Kwon, T. K. *Biochem. Biophys. Res. Commun.* **2004**, *325*, 1215.
10. Woo, K. J.; Yoo, Y. H.; Park, J. W.; Kwon, T. K. *Apoptosis* **2005**, *10*, 1333.
11. Lee, S. J.; Yoon, J. H.; Song, K. S. *Biochem. Pharmacol.* **2007**, *74*, 215.
12. Ramos, A. M.; Aller, P. *Biochem. Pharmacol.* **2008**, *75*, 1912.
13. Zhang, Q.; Zhao, X. H.; Wang, Z. J. *Food Chem. Toxicol.* **2008**, *46*, 2042.
14. Zhang, Q.; Zhao, X. H.; Wang, Z. J. *Toxicol in Vitro.* **2009**, *23*, 797.
15. Parajuli, P.; Joshee, N.; Rimando, A. M.; Mittall, S.; Yadav, A. K. *Planta Med.* **2009**, *75*, 41.
16. Wang, H. W.; Lin, C. P.; Chiu, J. H.; Chow, K. C.; Kuo, K. T.; Lin, C. S.; Wang, L. S. *Int. J. Cancer* **2007**, *120*, 2019.
17. Wang, W. Q.; VanAlstyne, P. C.; Irons, K. A.; Chen, S.; Stewart, J. W.; Birt, D. R. *Nutr. Cancer* **2004**, *48*, 106.
18. Khoo, B. Y.; Chua, S. L.; Balaran, P. *Int. J. Mol. Sci.* **2010**, *11*, 2188.
19. Kaplan, B. J.; Andrus, G. M.; Parish, W. W. *J. Altern. Complement Med.* **2004**, *10*, 345.
20. Choi, S.; Oh, C.; Han, J.; Park, J.; Choi, J. H.; Min, N. Y.; Lee, K. H.; Park, A. J.; Kim, Y. J.; Jang, S. J.; Lee, D. H. *Eur. J. Med. Chem.* **2010**, *45*, 1654.
21. Pi, J.; Zeng, J.; Luo, J. J.; Yang, P. H.; Cai, J. Y. *Bioorg. Med. Chem. Lett.* **2013**, *23*, 2902.
22. Nakamura, T.; Saito, M.; Aso, H. *Biosci. Biotechnol. Biochem.* **2012**, *76*, 375.
23. Aso, H.; Suzuki, F.; Yamaguchi, T.; Hayashi, Y.; Ebina, T.; Ishida, N. *Microbiol. Immunol.* **1985**, *29*, 65.
24. Nakamura, T.; Nagura, T.; Akiba, M.; Sato, K.; Tokuji, Y.; Ohnishi, M.; Osada, K. *J. Health Sci.* **2010**, *56*, 72.
25. Li, X. L.; Chen, T.; Wong, Y. S.; Xu, G.; Fan, R. R.; Zhao, H. L.; Chan, J. C. N. *Int. J. Biochem. Cell Biol.* **2011**, *43*, 525.
26. Li, J. J.; Tang, Q.; Li, Y.; Hu, B. R.; Ming, Z. Y.; Fu, Q.; Qian, J. Q.; Xiang, J. Z. *Acta Pharmacol. Sin.* **2006**, *27*, 1078.
27. Huang, C. H.; Jin, H.; Song, B.; Zhu, X.; Zhao, H. X.; Cai, J. Y.; Lu, Y. J.; Chen, B.; Lin, Y. C. *Appl. Microbiol. Biotechnol.* **2011**, *93*, 777.
28. Gottlieb, E.; Armour, S. M.; Harris, M. H.; Thompson, C. B. *Cell Death Differ.* **2003**, *10*, 709.
29. Lee, S. R.; Lo, E. H. *J. Cereb. Blood Flow Metab.* **2004**, *24*, 720.
30. Mattson, M. P.; Kroemer, G. *Trends Mol. Med.* **2003**, *9*, 196.
31. Qian, Y.; Wang, H.; Yao, W.; Gao, X. *Cell Biol. Int.* **2008**, *32*, 304.
32. Suva, L. J.; Griffin, R. J.; Makhoul, I. *Endocr. Relat. Cancer* **2009**, *16*, 703.
33. Charriaut, M. C.; Ben, A. Y. *NeuroReport* **1995**, *7*, 61.
34. Grzanka, A.; Grzanka, D.; Orlikowska, M. *Biochem. Pharmacol.* **2003**, *66*, 1611.
35. Olivia, N. T.; Jocelyne, H.; Jacqueline, B. *Biochem. Pharmacol.* **2008**, *76*, 11.
36. George, J.; Todaro, G. K.; Lazar, H. G. *J. Cell Physiol.* **1965**, *66*, 325.
37. Tiryaki, V. M.; Khan, A. A.; Ayres, V. M. *Scanning* **2012**, *34*, 316.
38. Kim, K. S.; Cho, C. H.; Park, E. K.; Jung, M. H.; Yoon, K. S.; Park, H. K. *PLoS ONE* **2012**, *7*, e30066.